Iranian Journal of Electrical and Electronic Engineering 03 (2020) 325–335
Special Issue on Smart Grids

Iranian Journal of Electrical and Electronic Engineering

Journal Homepage: ijeee.iust.ac.ir

Research Paper

Online Voltage Stability Monitoring and Prediction by Using Support Vector Machine Considering Overcurrent Protection for Transmission Lines

A. H. Poursaeed* and F. Namdari*(C.A.)

Abstract: In this paper, a novel method is proposed to monitor the power system voltage stability using Support Vector Machine (SVM) by implementing real-time data received from the Wide Area Measurement System (WAMS). In this study, the effects of the protection schemes on the voltage magnitude of the buses are considered while they have not been investigated in previous researches. Considering overcurrent protection for transmission lines not only resolves some drawbacks of the previous studies but also brings the case study system closer to the realities of actual systems. Online monitoring of system stability is performed by prediction of the Voltage Stability Index (VSI) and carried out by using Support Vector Regression (SVR). Due to the direct effect of appropriate SVR parameters on the prediction quality, the optimum value is chosen for learning machine hyperparameters using Differential Evolution (DE) algorithm. The obtained simulation results demonstrate high accuracy, effectiveness, and optimal performance of the proposed technique in comparison with Back-Propagation Neural Network (BPNN) and Adaptive Neuro-Fuzzy Inference System (ANFIS) approaches. The presented method is carried out on the 39 bus New England system.

Keywords: Voltage Stability, Support Vector Machine, Overcurrent Protection, Wide Area Measurement System, Differential Evolution.

1 Introduction

STABILITY always has been a fundamental issue in the field of power systems generation and transmission, which has become more complicated than ever before with the physical growth and parallel connection of the generators [1]. According to the recorded reports of the main reasons for worldwide blackouts in recent years, voltage instability is among the most serious threats to the safe operation of the power systems, [2]. Today, WAMS technology, with the aid of Phasor Measurement Units (PMUs), has enabled the monitoring of the dynamic model of the power system in real-time to improve the observability of power system stability status [3].

Iranian Journal of Electrical and Electronic Engineering, 2020.
Paper first received 31 October 2019, revised 24 March 2020, and accepted 10 April 2020.
* The authors are with the Department of Electrical Engineering, Lorestan University, Khorramabad, Iran.
E-mails: poursaeed.ah@fe.lu.ac.ir and namdari.f@lu.ac.ir.
Corresponding Author: F. Namdari.

Nowadays, with the increasing installation of PMUs in power systems, some Machine Learning techniques such as Artificial Neural Networks (ANN), Fuzzy Logic (FL), Decision Trees (DTs), ANFIS, and SVMs are used to assess voltage stability of the system. ANN has been used to estimate voltage stability status under normal and abnormal conditions [4] as well as to find the minimum input variables to fast estimation of the voltage stability margin with high accuracy [5, 6]. Reference [7] proposes a prediction of voltage stability margin using RBF neural network and performs feature extraction for the voltage profile of the buses using wavelet analysis and Principal Component Analysis (PCA). In [8], a functional estimation of steady-state voltage stability limits is proposed by calculating the critical values of the minimum singular values and the tangent vector norm using ANN. In [9], a voltage stability assessment criterion based on implementing of DT algorithm is proposed. According to a predetermined pattern and load-generation variation scenarios, continuous load flow calculations are performed. Then, the system is labeled as safe or unsafe

on each operating point of the system. Authors in [10] train a DT by reducing the dimension of the received data from WAMS using PCA. Then, the important branches through the feature selection technique are identified. Finally, the system security degree is determined. The application of FL to estimate the voltage magnitude of the load buses for every possible contingency is discussed in [11]. Reference [12] also measures the margin of the current operating point to the collapse point using ANFIS and an automatic voltage stability assessment tool. In [13], an estimation of the system loadability margin considering the uncertainty of the load with high accuracy using an ANFIS based on subtractive clustering has discussed. References [14-16], first calculate a voltage stability index, then predicts the values of the voltage stability indices using SVR. Also, SVR hyperparameters are optimized by GA, Dragonfly Optimization Algorithm (DOA), and Particle Swarm Optimization (PSO), respectively. GA has many disadvantages, such as adjustment for choosing appropriate operators and premature convergency. PSO also has many parameters to choose that affect the performance of the algorithm. However, DOA is easier to use than PSO and GA but has trouble in trapping to the local minimum. In [17], by performing online contingency analysis, three different indices are considered for each induction machine of the system. When a fault occurs, the time series of the induction machines slip is calculated using real-time data received from PMUs. Afterward, through the Least Square-Support Vector Machine (LS-SVM), time series prediction is performed and the voltage instability index is predicted by slip trajectory monitoring. Although LS-SVM has a lower computational burden than SVM and solves a linear programming problem instead of a quadratic programming problem, but it has loss of sparseness. Reference [18] also addresses the use of SVM in voltage stability prediction and monitoring for distribution systems and the advantage of PSO based SVM over GA-SVM. The Prediction of the load margin using real-time data from PMUs using SVR has been studied in [19]. Due to its higher speed of the mentioned method compared to others, control actions can be taken early to prevent voltage collapse. Also with the injection of reactive power into the weakest buses by FACTS devices, voltage stability status could be improved. The main drawback of this paper is that it compares the different methods without tuning their hyperparameters, while the proper selection of these quantities has a direct impact on the prediction process. The mentioned papers have not considered the effect of the protection systems on voltage monitoring of the actual systems. The operation of the protective relays changes the configuration of the system under normal conditions. Since the protection system operation causes a step transition in the system graph (i.e. a line outage due to relay operation causes a step change in the measurements), in this study these binary effects of the protective relays on the nonlinear system have been considered. Also, previous studies are not applicable to the online prediction of voltage stability while the proposed method is tested online and is compatible with Wide Area Monitoring, Protection and Control (WAMPAC) system.

This paper has considered the effect of the protective relay operations on voltage stability while the previous studies do not. Then, a comprehensive scheme is proposed to online monitoring and predicting of voltage stability using a DE based SVR (DE-SVR). In the presented scheme, overcurrent protection is considered for the transmission lines of the system under study. Optimal coordination of Directional Overcurrent Relays (DOCRs) has also been established by implementing the Genetic Algorithm (GA). Then, a time-domain based index is considered to evaluate the voltage stability status of this proposed scheme which is predicted by SVR. To improve the accuracy of the prediction, the hyperparameters of this learning machine are obtained using the DE algorithm. DE has less parameter to adjust, high convergence speed and it is easy to implement. Finally, the results of the proposed method are discussed and compared with BPNN and ANFIS. The proposed method has been implemented on the 39 bus New England system.

The rest of the paper organized as follows. Section 2 describes the index of voltage stability assessment and optimal coordination of DOCRs. Section 3 investigates the structure of SVMs and SVRs. Section 4 presents the proposed method. Section 5 is simulation results and discussion about comparison of the proposed method with BPNN and ANFIS approaches. Finally, the conclusion represents in Section 6.

2 Problem Formulation

2.1 Voltage Stability Assessment

Voltage stability refers to the ability of the system to maintain the voltage magnitude of all of the buses at an acceptable steady-state value in whether normal or abnormal operating conditions. Numerous studies have been conducted to evaluate the system voltage stability by providing various indices [20]. In [21], a voltage stability index using real-time data received from WAMS has been introduced. This index called Voltage Stability Index (VSI) and measures the voltage stability margin. Also, one of the voltage stability evaluation indices is defined for the transmission lines of the power system. The basis for the calculation of VSI is based on the simple two-stroke power system as shown in Fig. 1.

The VSI is defined as (1):

$$VSI = \min\left(\frac{P_{\text{margin}}}{P_{\max}}, \frac{Q_{\text{margin}}}{Q_{\max}}, \frac{S_{\text{margin}}}{S_{\max}}\right) \quad (1)$$

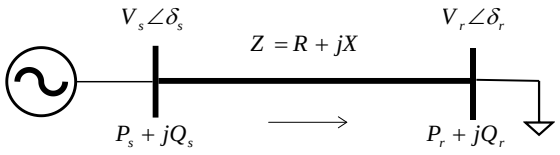

Fig. 1 Two bus power system.

where P_{margin}, Q_{margin}, and S_{margin} are the margins of active, reactive, and apparent power at the end of the line (receiving end), respectively. These parameters are defined as (2)-(4).

$$P_{\text{margin}} = P_{\max} - P_r \tag{2}$$

$$Q_{\text{margin}} = Q_{\max} - Q_r \tag{3}$$

$$S_{\text{margin}} = S_{\max} - S_r \tag{4}$$

where $P_{\max}$, $Q_{\max}$, and $S_{\max}$ are the maximum active, reactive, and apparent power at the end of the line, respectively, as well as P_r, Q_r, and S_r are the active, reactive, and apparent power received at the receiving end. These parameters are also expressed as (5)-(10).

$$P_{\max} = \sqrt{\frac{V_s^4}{4X^2} - Q_r\frac{V_s^2}{X}} \tag{5}$$

$$Q_{\max} = \frac{V_s^2}{4X} - \frac{P_r^2 X}{V_s^2} \tag{6}$$

$$S_{\max} = \frac{\left(1-\sin\left(\arctan\frac{Q_r}{P_r}\right)\right)V_s^2}{2\cos\left(\arctan\frac{Q_r}{P_r}\right)^2 X} \tag{7}$$

$$P_r = \left[\left(V_s\cos(\delta_s-\delta_r)-V_r\right)\frac{R}{R^2+X^2} + V_s\sin(\delta_s-\delta_r)\frac{X}{R^2+X^2}\right]V_r \tag{8}$$

$$Q_r = \left(V_s\cos(\delta_s-\delta_r)-V_r\right)\frac{X}{R^2+X^2} - V_s\sin(\delta_s-\delta_r)\frac{R}{R^2+X^2}\Bigg]V_r \tag{9}$$

$$S_r = P_r + jQ_r \tag{10}$$

VSI is considered stable if it is greater than zero (positive value) and when the value equal to zero, the system will go to the voltage collapse point.

2.2 Overcurrent Protection

One of the major effects of the fault in the power system is the occurrence of a sudden large current that flows through the system. Therefore, the amplitude of the current can be used as one of the signs of the incident of a fault in the system. So overcurrent protection is one of the most efficient protection schemes that is widely used in power systems as primary and backup protection.

2.2.1 Optimal Coordination of the Directional Overcurrent Relays

Optimal coordination of DOCRs for their fast and efficient performance is a very important issue. Coordination of the protection relays means choosing the right settings for the relays so that their protection function meets the requirements of a protection system under different conditions. These features include sensitivity, selectivity, reliability, and speed. Choosing valid settings for the relays plays a very important role in reducing and isolation of the effect of the faults on the system.

Many studies have been conducted on the problem of optimal coordination using mathematical methods, artificial intelligence-based methods, and a combination of these two approaches [22]. In recent years, optimal coordination of DOCRs with Quadratic Constrained Quadratic Programming (QCQP) [23], Mixed Integer Linear Programming (MILP) [24], Biogeography-Based Optimization-Linear Programming (BBO-LP) [25], Gravitational Search Algorithm-Sequential Quadratic Programming (GSA-SQP) [26] and the hybrid heuristic methods such as Gravitational Search Algorithm-Particle Swarm Optimization (PSO-GSA) [27] have also been solved. Reference [28] proposed a new objective function to optimally solve the DOCRs coordination problem that addresses the problems of miscoordination between primary and backup relays and the larger operating time of backup relays in previous studies has resolved.

The general form of Inverse Definite Minimum Time (IDMT) overcurrent relay operating time is defined by IEC 60255 and IEEE C37.112 [29], and is given in (11):

$$t_i = \frac{\alpha(TMS_i)}{\left(\frac{I_{f_i}}{I_{pu_i}}\right)^{\beta} - 1} + \gamma \tag{11}$$

where t_i is operating time the relay i, and TMS_i and I_{pui} are time multiplier setting and pickup current of the relay i, respectively. Also, I_{fi} is the fault current passing through the main relay, α, β, and γ are the constant values. Table 1 provides the constant values of the parameters for curves defined by IEEE C37.112 and IEC 60255.

The most commonly used objective function of the optimal coordination problem of DOCRs (OF1) for a sample power system as shown in Fig. 2, expressed

Table 1 IEEE and IEC constants for standard DOCRs.

IDMT Curve	α		β		γ	
	IEEE	IEC	IEEE	IEC	IEEE	IEC
Moderately (standard) inverse	0.0515	0.14	0.02	0.02	0.114	0
Very inverse	19.61	13.5	2	1	0.491	0
Extremely inverse	28.2	80	2	2	0.1217	0

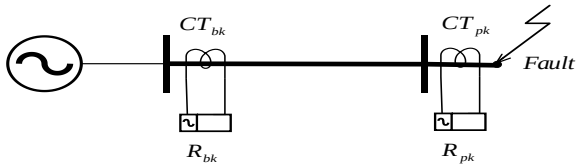

Fig. 2 Sample power system.

in (12). This equation is standard inverse IDMT of the IEC standard for DOCRs. The objective is to minimize the operating times of all main relays.

$$OF1 = \sum_{i=1}^{m} t_i = \sum_{i=1}^{m} \left(\frac{0.14 \times TMS_i}{\left(\frac{I_{f_i}}{I_{pu_i}} \right)^{0.02} - 1} \right) \tag{12}$$

where m is the total number of main relays. The result of optimizing the objective functions of the optimal coordination of DOCRs is to calculate the optimal value for the problem decision variables *TMS* and I_{pu}. These decision variables are also bounded and form the constraints of the coordination problem in (13) and (14):

$$0.1 \le TMS_i \le 1.1 \tag{13}$$

$$1.25 I_{l_{\max_i}} \le I_{pu_i} \le \frac{2}{3} I_{f_{\min_i}} \tag{14}$$

where, in (13) and (14), $I_{l_{\max_i}}$ is the maximum load current and $I_{f_{\min_i}}$ is the minimum fault current pass through the relay i.

The proposed objective function in [28], namely POF, is defined to overcome the problems of similar studies in (15):

$$POF = \alpha_1 \sum_{i=1}^{m} t_i^{\,2} + \alpha_2 \sum_{k=1}^{n} \left(\left| \Delta t_{pbk} - \left| \Delta t_{pbk} \right| \right| \frac{t_{pk}^2}{t_{bk}^2} + \left(\Delta t_{pbk} + \left| \Delta t_{pbk} \right| \right) t_{bk}^2 \right) \tag{15}$$

where n is the number of primary and backup relay pairs, t_{pk} and t_{bk} are the operating time of the primary and backup relay for the relay pairs k, respectively. In the end, α_1 and α_2 are control parameters to control over both terms in (15). In POF, these two weight factors are considered 1. Also Δt_{pbk}, the discrimination time between the relay pairs k, expressed as (16):

$$\Delta t_{pbk} = t_{bk} - t_{pk} - CTI \tag{16}$$

where *CTI* is the coordination time interval which is assumed 0.2 seconds in this article. Negative values of Δt_{pbk} indicate that the primary relays have a longer operating time than the backup ones, which may cause miscoordination in the protection system. It should be noted that the computation of Δt_{pbk} for all relay pairs is intended both for fault occurring at the near-end terminal and faults at the far-end terminal.

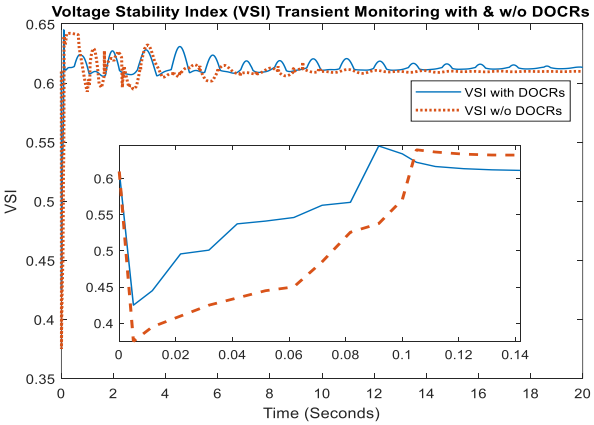

Fig. 3 Transient Monitoring of VSI in the presence and absence of overcurrent protection.

Due to the nonlinear nature of this objective function, GA is used to minimize POF and then obtain optimal values for decision variables.

2.3 Analysis of the Effect of Considered Overcurrent Protection for Transmission Lines on Voltage Stability

A case study is used to describe the effect of considering overcurrent protection for transmission lines on voltage stability. VSI transient monitoring due to a three-phase short circuit fault occurred at 50% of the transmission line between bus 2 and bus 3 at zero second and its clearance at 0.1 second are examined in the presence and absence of overcurrent protection in Fig. 3. Also, the time interval between 0 to 0.15 seconds is enlarged for better clarity and a description of what happened.

3 Support Vector Machine

Support vector machine is a machine learning technique for the classification of two or more groups of problems. SVM maps nonlinear inputs vectors to a high dimensional feature space. SVM is based on Structural Risk Minimization (SRM) while the neural networks minimize the classification errors [30].

3.1 Support Vector Regression

Support vector regression is an extended model of SVM for the function estimation problem, as shown in Fig. 4 [31]. The SVR estimates the function $f(x)$ with the training data. These data are defined as $\{(x_1, y_1), \ldots, (x_n, y_n)\}$, $x_i \in \mathbb{R}^m$, where x_i, y_i, and n are the input data sets, output data sets, and the total number of the samples, respectively. To estimate voltage stability, x_i includes voltage magnitude and reactive power for the parameter i, while y_i is the VSI value for the data i.

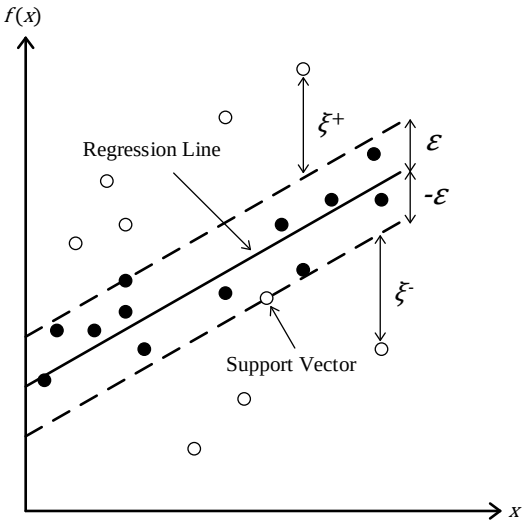

Fig. 4 Support vector regression.

Therefore, SVR predicts output values using the regression function according to (17):

$$f\left(x\right)=\omega^{T}.\varphi\left(x\right)+b \tag{17}$$

where $f(x)$ is the predicted output value, $\varphi(x)$ is the high-dimensional input vector, ω is the weight vector while b considered as the bias. By minimizing the risk function expressed in (18), ω and b coefficients are calculated.

$$R_{reg}\left[f\right]=C\frac{1}{n}\sum_{i=1}^{n}L\left(y_i,f\left(x_i\right)\right)+\frac{1}{2}\left\|\omega\right\|^{2} \tag{18}$$

where C is a predetermined coefficient that measures the empirical risk. Also, C can play a role as a penalty factor when the fault occurs and make balances between the empirical risk and the second term in (18). Also, L is a loss function expressed as (19):

$$L\left(y_i,f\left(x_i\right)\right)=\begin{cases}\left|f\left(x_i\right)-y_i\right|-\varepsilon, & \text{if } \left|f\left(x_i\right)-y_i\right|\geq\varepsilon\\ 0, & \text{otherwise}\end{cases} \tag{19}$$

In this loss function, which is known as *ε–Insentive*, ε represents the range between the actual values and the values of the regression function specified in Fig. 3. This problem does not allow any errors, so in order to include the training error (exterior data of ε tube), ξ_i^{+} and ξ_i^{-} are used as two slack variables (which is shown in Fig. 3) is used. The optimization problem is expressed as (20) which is bounded by constraints in (21):

$$\min\left\{R_{reg}\left[\omega,\xi\right]=C\frac{1}{n}\sum_{i=1}^{n}(\xi_i^{+}+\xi_i^{-})+\frac{1}{2}\left\|\omega\right\|^{2}\right\} \tag{20}$$

$$\left\{\begin{array}{c}\omega.\varphi(x)+b-f\left(x_i\right)\leq\varepsilon+\xi_i^{-}\\ f\left(x_i\right)-(\omega.\varphi(x)+b)\leq\varepsilon+\xi_i^{+}\\ \xi_i^{-},\xi_i^{+}\geq 0\end{array}\right\},i=1,2,...,n \tag{21}$$

The dual problem of (20) is defined as (22) which is bounded by constraints presented in (23):

$$\max\left\{-\frac{1}{2}\sum_{i,j=1}^{n}(\alpha_i^{-},\alpha_i^{+})(\alpha_i^{-},\alpha_i^{+})\left(k\left(x_i,x_j\right)\right)-\varepsilon\sum_{i=1}^{n}(\alpha_i^{-},\alpha_i^{+})+\sum_{i=1}^{n}y_i\left(\alpha_i^{-},\alpha_i^{+}\right)\right\} \tag{22}$$

$$\left\{\begin{array}{c}\sum_{i=1}^{n}(\alpha_i^{-}-\alpha_i^{+})=0\\ 0\leq\alpha_i^{-}\leq C\\ 0\leq\alpha_i^{+}\leq C\end{array}\right\},i=1,2,...,n \tag{23}$$

where α_i^{-} and α_i^{+} are lagrangian multipliers, which solve the quadratic problem expressed in (23) and bring the predicted values closer to the actual values. Also, $k(x_i, x_j)$ is a kernel function that is calculated by the vector product of $\varphi(x_i)$ and $\varphi(x_j)$ in the feature space. The kernel function used in this study is the Gaussian kernel function described in (24):

$$k\left(x_i,x_j\right)=\exp\left(\frac{-\left\|x_i-x_j\right\|^{2}}{2\sigma^{2}}\right) \tag{24}$$

where σ^2 is the bandwidth of Gaussian kernel function. In this study, C, σ^2, and ε obtained by using the DE algorithm.

4 The Proposed Method

First, the optimal coordination of overcurrent relays is performed. The optimal settings for *TMS* and I_{pu} are obtained by using GA according to the procedure described in Fig. 5.

First, primary/backup relay pairs are determined. Then, the initial population is generated, and accordingly, *TMS* and I_{pu} are assigned a value. Given these values, the fitness function is evaluated. Next, the GA selection operator is determined. Finally, GA crossover and mutation operators are applied to the population, respectively. If the stop criteria are satisfied, the optimal values for *TMS* and I_{pu} are obtained. The assumed parameters for GA are shown in Table 2.

In this paper, we assume that the data is received from the PMUs installed in the understudy system to make it observable. The flowchart of the proposed method is shown in Fig. 6. By using these data corresponds to

Table 2 GA parameter settings.

Parameters	Settings
Generations	1000
Population size	100
Cross-over rate	0.95
Mutation rate	0.01
Selection type	Standard roulette wheel

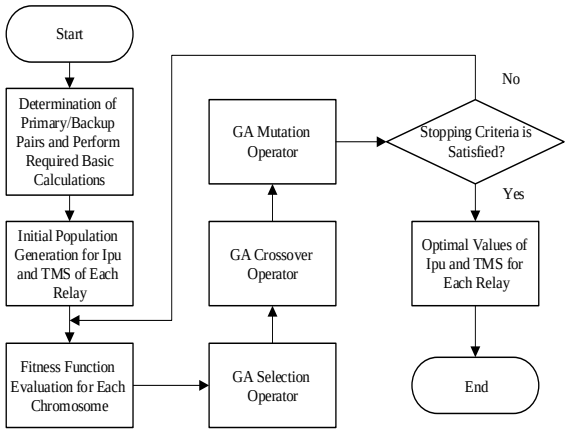

Fig. 5 Optimal coordination of DOCRs using GA flowchart.

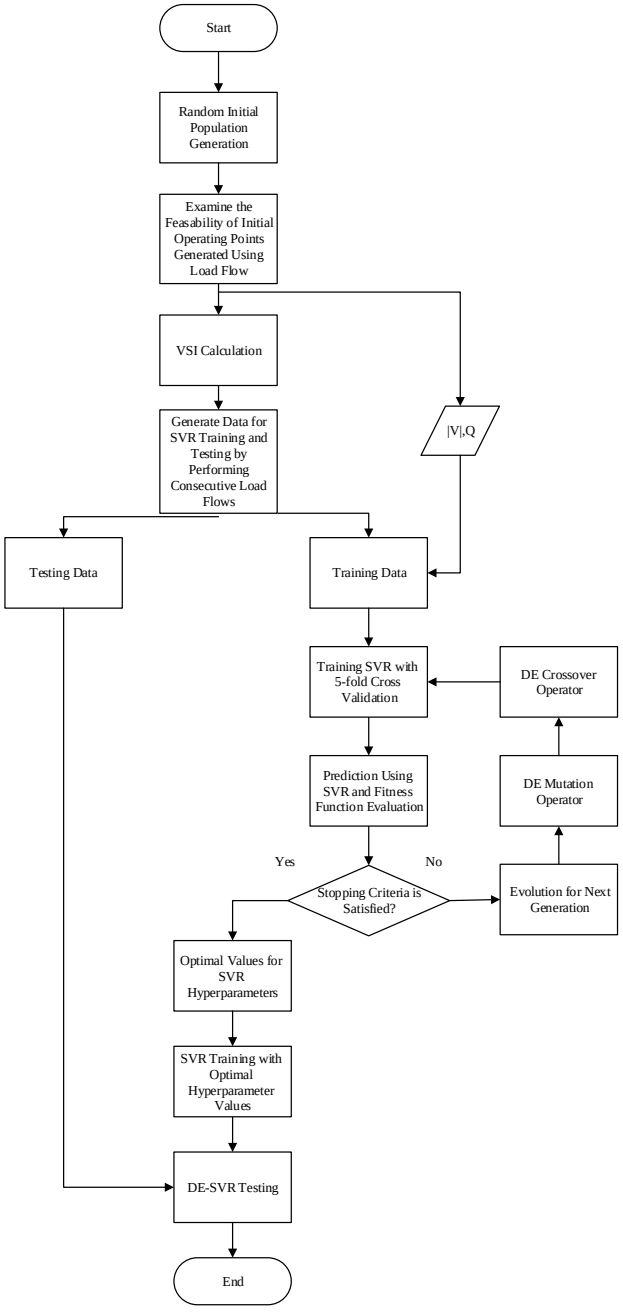

Fig. 6 Flowchart of the proposed method.

each load flow, the VSI is calculated and considered to be the actual value. Also, the values of the voltage magnitudes and reactive power of the buses are considered as inputs to the DE-SVR. Then, using the DE algorithm [33], the SVR hyperparameters, C, σ^2, and ε are fixed at their optimal value. In this paper, 5-fold cross-validation is used for training data. In this technique, 80% of the data is considered as training data sets, and then the performance of SVR is evaluated on the remaining 20% of the data.

The minimization objective function by using the DE method is the MSE function that expressed in (25):

$$\min\left\{MSE = \frac{1}{n}\sum_{i=1}^{n}\left(y_i - y_{p_i}\right)^2\right\} \tag{25}$$

where n, y_i, and y_{p_i} are the number of samples, the actual values, and the predicted values, respectively. The setting parameters of the DE algorithm and the limits of the SVR hyperparameters are presented in Table 3.

To compare the performance of prediction accuracy three performance evaluation indices MSE, RMSE, and MAE are used which are defined in (26) to (28), respectively. The smaller the value of these indices (near zero) leads the higher the prediction accuracy.

$$MSE = \frac{1}{n}\sum_{i=1}^{n}\left(y_i - y_{p_i}\right)^2 \tag{26}$$

$$RMSE = \sqrt{\frac{1}{n}\sum_{i=1}^{n}\left(y_i - y_{p_i}\right)^2} \tag{27}$$

$$MAE = \frac{1}{n}\sum_{i=1}^{n}\left|y_i - y_{p_i}\right| \tag{28}$$

Another performance index, called the correlation index or R, is defined, which is defined by (29):

$$R = \frac{\sum_{i=1}^{n}\left(y_i - \bar{y}\right)\left(y_{p_i} - \overline{y_p}\right)}{\sqrt{\sum_{i=1}^{n}\left(y_i - \bar{y}\right)^2\left(y_{p_i} - \overline{y_p}\right)^2}} \tag{29}$$

where $\bar{y}$ and $\overline{y_p}$ are rates of the actual and predicted values, respectively. The closer the value of this index to 1 leads to the higher the prediction accuracy.

Table 3 Setting parameters of the DE algorithm.

Parameter	Setting
Generations	100
Population size	40
Scale factor	0.1-0.9
Crossover rate	0.3
C	0.1-1000
σ^2	0.1-1000
ε	0.00001-0.1

5 Results

To demonstrate the effectiveness of the DE-SVR method for online monitoring and prediction of power system voltage stability, the proposed method is applied to the 39 bus New England system. The understudy system, as shown in Fig. 7, comprises 39 buses, 10 generators, 19 loads, and 34 transmission lines. The available DOCRs in transmission lines painted in red to simply distinguish from other equipments.

5.1 Optimal Coordination of DOCRs Using GA

Optimal coordination of DOCRs is done by GA and the optimal settings for *TMS* and I_{pu} are obtained. The optimal value obtained for POF using GA is 35.2891, while optimal values of the decision variables *TMS* and I_{pu} are addressed in the Appendix and Table A.1. The convergence diagram of the objective function using GA is shown in Fig. 8.

5.2 The Optimum Values of SVR Hyperparameters Using DE

The results of the DE-SVR method are compared with the ANFIS and BPNN methods with the same data set for all three models. To generating of training 900 consecutive and different load flows ranged from 0.7 times the nominal load to 1.25 times the nominal load performed so that load flow does not diverge. Consecutive load flow is done by using MATPOWER toolbox in the MATLAB environment [32]. These 900 data sets randomly are used as training data and 100 data sets of unseen data through a time-domain study, are used as testing data. Also, in previous papers, SVM testing phases were done offline, so the prediction performance was unknown in real-time. In this study, the testing phase is done online. Therefore, the proposed scheme can be implemented in real-time for online applications in power systems.

Also, the results of optimization for SVR parameters are shown in Table 4 and the DE convergence diagram in Fig. 9.

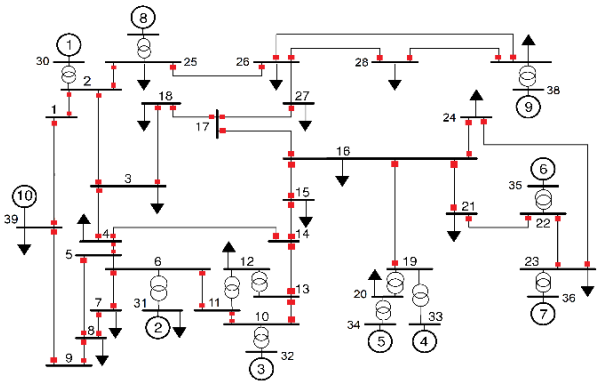

Fig. 7 39 bus New England system.

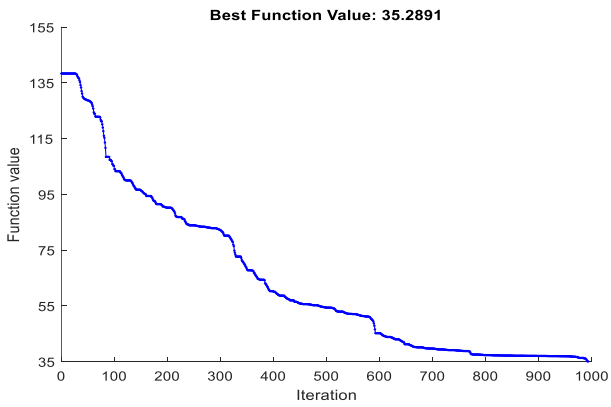

Fig. 8 Convergence diagram of POF using GA.

5.3 Comparison of Results and Discussions

In this section, the prediction accuracy of DE-SVR is compared with BPNN [14], [15] and ANFIS [16] approaches.

a) The BPNN or multilayered perceptron back propagation neural network is the most widely used neural network to solve nonlinear problems including one input layer, one or more hidden layers, and one output layer. This neural network is trained for up to a maximum epoch 100 or when the MSE value is less than 0.001. A training rate of 0.01 and a momentum constant of 0.9 have been assumed for this neural network. In this paper, 2 hidden layers considered while 5 neurons are assumed. It should be noted that the activation function used in this article is the Sigmoid function.

b) ANFIS or adaptive neural-fuzzy inference system that integrates the fuzzy system with an artificial neural network to improve the learning process. The most important factor in ANFIS design is the choice of the Fuzzy Inference System (FIS). In this paper, the subtractive clustering method is used to generate fuzzy rules. Also, the radius of influence in this study is considered to be 0.4.

The comparison between the actual and predicted

Table 4 Optimal values of SVR hyperparameters using DE.

Method	Hyperparameters SVR			Fitness function value
	C	σ^2	ε	
DE-SVR	41.6914	0.6645	2.4093e-4	4.1257e-5

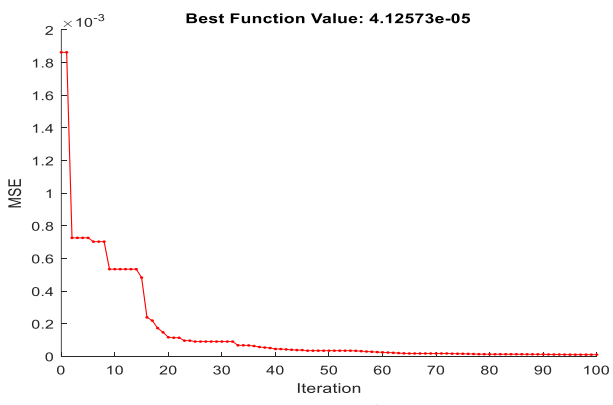

Fig. 9 Convergence Diagram of MSE using DE.

values by the DE-SVR, ANFIS and BPNN models for training data is shown in Fig. 10. The comparison of performance indices for all three methods is shown in Table 5 for the training data to predict VSI.

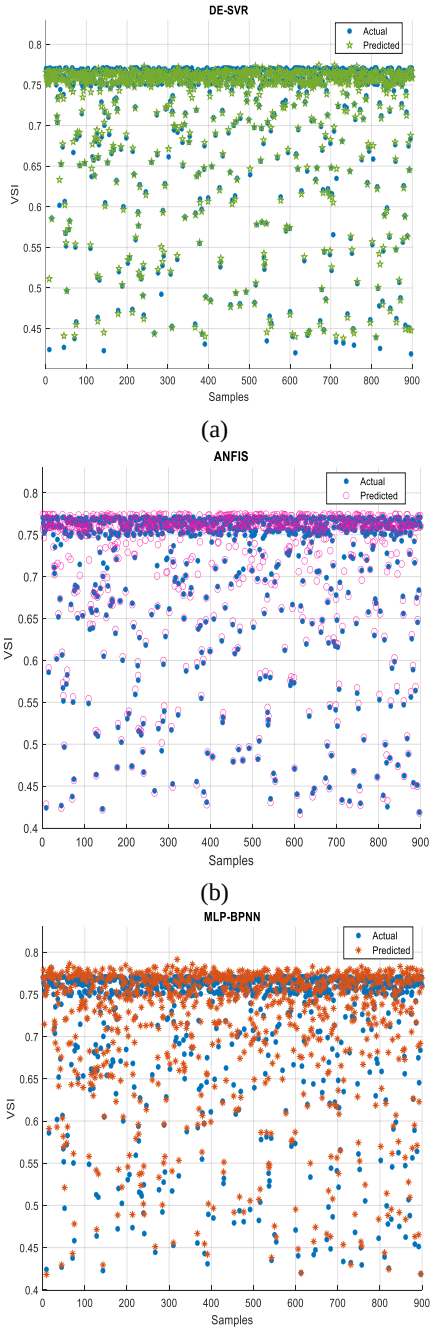

Fig. 10 Comparison between the actual values and predicted ones of VSI in training data: a) DE-SVR, b) ANFIS, and c) BPNN.

Table 5 Performance Indices for training data to predict VSI.

Performance Index	Training Data		
	DE-SVR	ANFIS	BPNN
MSE	4.1257e-5	5.1544e-5	3.4171e-4
RMSE	0.0064	0.0071	0.0184
MAE	0.0044	0.0039	0.0137

To generate the testing data, a time-domain study is performed in 0 to 0.1 second time interval with the changes in the static loads in the 39 bus system. The time step for the time-domain simulation is equal to 0.001 seconds. Based on these testing data, the online prediction has been performed by using the proposed methods DE-SVR, ANFIS, and BPNN. A comparison between actual and predicted VSI values in all three methods is shown in Fig. 11.

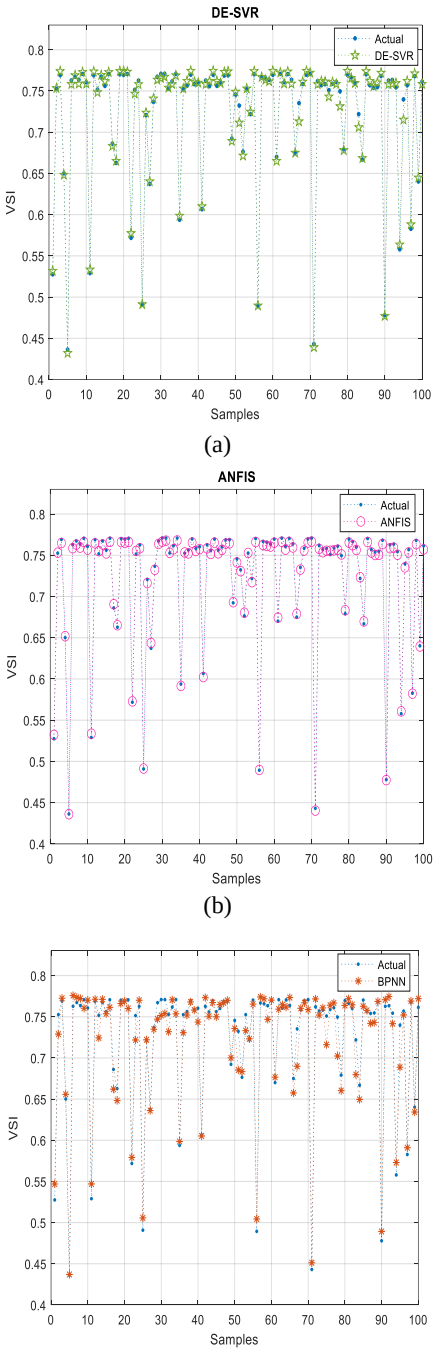

Fig. 11 Comparison between the actual value and predicted ones of VSI in testing data: a) DE-SVR, b) ANFIS, and c) BPNN.

The comparison of performance indices for all three methods is shown in Table 6 for the testing data to predict VSI.

Table 6 Performance Indices for testing data to predict VSI.

Performance Index	Training Data		
	DE-SVR	ANFIS	BPNN
MSE	5.2746e-5	5.4631e-5	1.2404e-3
RMSE	0.0072	0.0073	0.0352
MAE	0.0046	0.0042	0.0151

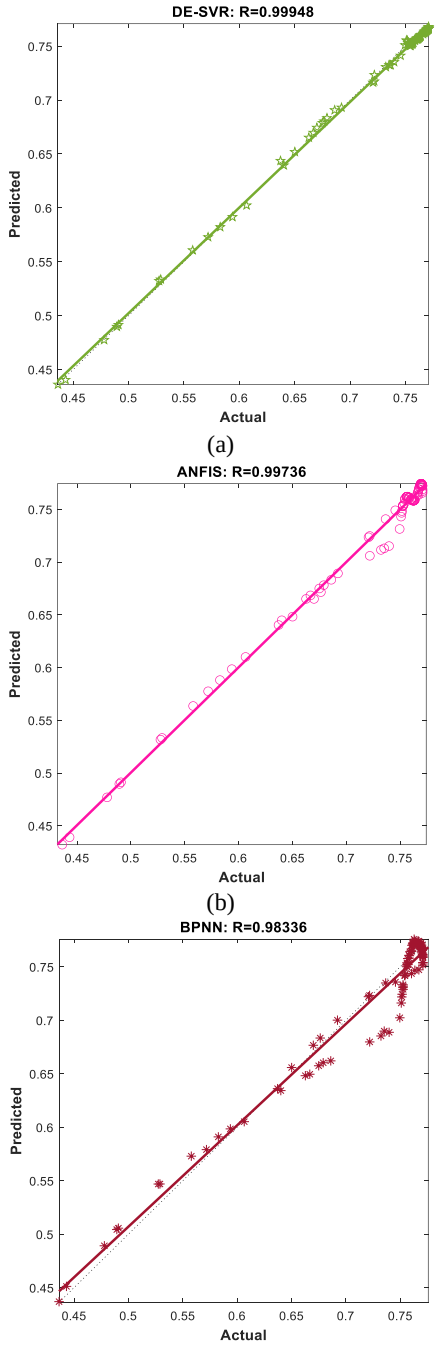

Fig. 12 Comparison between correlation diagram of actual values vs. predicted values in testing data: a) DE-SVR, b) ANFIS, and c) BPNN.

As shown in Tables 5 and 6, the DE-SVR method has higher prediction accuracy due to the smaller performance indices compared to other mentioned approaches either in the training data and the testing data.

The correlation diagram of the actual values vs. the predicted values for the testing data is shown in Fig. 12. Since it can be seen in Fig. 12 and the upper part of each section, the performance of the proposed method is better than the other methods in predicting VSI values in the testing data.

The comparison of the correlation index for all of the three methods is shown in Table 6 for the testing data to predict VSI. As shown in Table 7, the correlation index for DE-SVR is near to 1 that shows the better performance to predict the VSI than the other approaches.

5.4 Comparison between Training and Testing Time

The computer with specification Intel® Core™ i7-4510U CPU @ 2 GHz calculates the training and testing time of each method. All methods are trained and tested on the same computer with the same data set. The results are shown in Table 8.

As can be seen, the proposed method takes less time to be trained and tested, which is indicated that the proposed method is faster than other approaches.

6 Conclusion

In this paper, a method for online predicting and monitoring the system voltage stability with consideration of overcurrent protection for transmission lines using DE-based SVR has been proposed. The voltage magnitudes and reactive power of the buses are used as inputs to the DE-SVR to estimate the VSI. The performance of the proposed method on the 39 bus New England system is discussed. The results show that the DE-SVR method has advantages over ANFIS and BPNN methods. MSE of DE-SVR is 5.2746e-5 that is indicative of its higher accuracy than other approaches. The correlation index of the proposed method on test data is 0.99948, i.e. there is a strong correlation between the actual values and the predicted ones. Also, in terms of training and testing times, the presented approach is superior to the other methods, with 0.8573 and 0.0062 seconds, respectively.

Table 7 Correlation index for testing data to predict VSI.

Method	*R*
DE-SVR	0.99948
ANFIS	0.99736
BPNN	0.98336

Table 8 Comparison between training and testing times.

Method	Training time [s]	Testing time [s]
DE-SVR	0.8573	0.0062
ANFIS	1.1696	0.0084
BPNN	1.3575	0.0105

Appendix

Table A.1 Optimal Values of *TMS* and I_{pu} for all of the available relays.

Relay	*TMS*	I_{pu}	Relay	*TMS*	I_{pu}
OC01-02	0.1	1005.71	OC15-16	0.1684	705.175
OC01-39	0.1399	665.879	OC16-15	0.1514	692.267
OC02-01	0.1356	2211.71	OC16-17	0.1	2894.28
OC02-03	0.1	3368.24	OC16-19	0.1	1882.13
OC02-25	0.2376	505.609	OC16-21	0.1	2112.43
OC03-02	0.1001	2168.8	OC16-24	0.1	2586.69
OC03-04	0.1	3225.61	OC17-16	0.1	1888.34
OC03-18	0.1922	828.53	OC17-18	0.1	1970.63
OC04-03	0.1055	1647.56	OC17-27	0.149	1771.62
OC04-05	0.2194	574.36	OC18-03	0.3694	164.313
OC04-14	0.1	4209.55	OC18-17	0.1078	1482.36
OC05-04	0.1	5297.75	OC19-16	0.1238	1071.93
OC05-06	0.1576	966.82	OC21-16	0.1	1407.88
OC05-08	0.2322	672.404	OC21-22	0.1	1550.82
OC06-05	0.1	4248.79	OC22-21	0.1066	1255.49
OC06-07	0.2314	899.853	OC22-23	0.3146	140.675
OC06-11	0.1617	1229.87	OC23-22	0.1328	812.003
OC07-06	0.1	1860.12	OC23-24	0.1177	1407.09
OC07-08	0.3277	391.117	OC24-16	0.2762	135.271
OC08-05	0.1047	2426	OC24-23	0.1	3014.9
OC08-07	0.3027	391.508	OC25-02	0.1732	558.29
OC08-09	0.3701	238.07	OC25-26	0.2123	485.634
OC09-08	0.1429	1503.85	OC26-25	0.2902	169.779
OC09-39	0.2863	159.31	OC26-27	0.213	553.132
OC10-11	0.1	3639.21	OC26-28	0.1614	1326.31
OC10-13	0.1112	2173.22	OC26-29	0.1	2643.23
OC11-06	0.2556	758.015	OC27-17	0.3553	68.8275
OC11-10	0.1007	2345.61	OC27-26	0.3084	570.963
OC13-10	0.1	1612.96	OC28-26	0.181	869.562
OC13-14	0.1	1612.95	OC28-29	0.114	695.826
OC14-04	0.1451	993.123	OC29-26	0.1	1832.33
OC14-13	0.1284	1259.91	OC29-28	0.1	2250.1
OC14-15	0.1	2143.11	OC39-01	0.1	1713.57
OC15-14	0.3547	61.1571	OC39-09	0.1	2341.92

References

[1] P. Kundur, *Power system stability and control*. McGraw-Hill Education, 1994.

[2] M. Eremia and M. Shahidehpour, *Handbook of electrical power system dynamics: Modeling, stability, and control*. IEEE Press, Wiley Publishing, 2013.

[3] A. G. Phadke and J. S.Thorp, *Synchronized phasor measurements and their applications*, Springer, 2008.

[4] D. Q. Zhou, U. D. Annakkage, and A. D. Rajapaks, "Online monitoring of voltage stability margin using an artificial neural network," *IEEE Transactions on Power Systems*, Vol. 25, No. 3, pp. 1566–1574, Aug. 2010.

[5] A. R. Bahmanyar and A. Karami, "Power system voltage stability monitoring using artificial neural networks with a reduced set of inputs," *International Journal of Electrical Power & Energy Systems*, Vol. 58, pp. 246–256, Jun. 2014.

[6] S. M. Ashraf, A. Gupta, D. K. Choudhary, and S. Chakrabarti, "Voltage stability monitoring of power systems using reduced network and artificial neural network," *International Journal of Electrical Power & Energy Systems*, Vol. 87, pp. 43–51, May 2017.

[7] S. Hashemi and M. R. Aghamohammadi, "Wavelet based feature extraction of voltage profile for online voltage stability assessment using RBF neural network," *International Journal of Electrical Power & Energy Systems*, Vol. 49, pp. 86–94, Jul. 2013.

[8] G. G. Lage, R. A. S. Fernandes, and G. R. M. da Costa, "Functional approximation of power system steady-state voltage stability limits by artificial neural networks," *Journal of Control, Automation and Electrical Systems*, Vol. 24, No. 4, pp. 544–554, Aug. 2013.

[9] M. Beiraghi and A. M. Ranjbar, "Online voltage security assessment based on wide-area measurements," IE*EE Transactions on Power Delivery*, Vol. 28, No. 2, pp. 989–997, Apr. 2013.

[10] H. Mohammadi and M. Dehghani, "PMU based voltage security assessment of power systems exploiting principal component analysis and decision trees," *International Journal of Electrical Power & Energy Systems*, Vol. 64, pp. 655–663, Jan. 2015.

[11] M. Ramaswamy and K. R. Nayar, "On-line estimation of bus voltages based on fuzzy logic," *International Journal of Electrical Power & Energy Systems*, Vol. 26, No. 9, pp. 681–684, Nov. 2004.

[12] A. Berizzi, C. Bovo, D. Cirio, M. Delfanti, M. Merlo, and M. Pozzi, "Online fuzzy voltage collapse risk quantification," *Electric Power Systems Research*, Vol. 79, No. 5, pp. 740–749, May 2009.

[13] S. P. Torres, W. H. Peralta, and C. A. Castro, "Power system loading margin estimation using a neuro-fuzzy approach," *IEEE Transactions on Power Systems*, Vol. 22, No. 4, pp. 1955–1964, Nov. 2007.

[14] K. S. Sajan, V. Kumar, and B. Tyagi, "Genetic algorithm based support vector machine for on-line voltage stability monitoring," *International Journal of Electrical Power & Energy Systems*, Vol. 73, pp. 200–208, Dec. 2015.

[15] G. S. Naganathan and K. Babulal, "Optimization of support vector machine parameters for voltage stability margin assessment in the deregulated power system," *Soft Computing*, pp. 1–13, Oct. 2018.

[16] M. Amroune, T. Bouktir, and I. Musirin, "Power system voltage stability assessment using a hybrid approach combining dragonfly optimization algorithm and support vector regression," *Arabian Journal for Science and Engineering*, Vol. 43, No. 6, pp. 3023–3036, Jun. 2018.

[17] H. Yang, W. Zhang, J. Chen, and L. Wang, "PMU-based voltage stability prediction using least square support vector machine with online learning," *Electric Power Systems Research*, Vol. 160, pp. 234–242, Jul. 2018.

[18] A. Shukla, K. Verma, and R. Kumar, "Online voltage stability monitoring of distribution system using optimized support vector machine," in *IEEE 6th International Conference on Power Systems (ICPS)*, New Delhi, pp. 1–6, 2016.

[19] M. V. Suganyadevi, C. K. Babulal, and S. Kalyani, "Assessment of voltage stability margin by comparing various support vector regression models," *Soft Computing*, Vol. 20, No. 2, pp. 807–818, Feb. 2016.

[20] J. Modarresi, E. Gholipour, and A. Khodabakhshian, "A comprehensive review of the voltage stability indices," *Renewable and Sustainable Energy Reviews*, Vol. 63, pp. 1–12, Sep. 2016.

[21] Y. Gong, N. Schulz, and A. Guzmán, "Synchrophasor-based real-time voltage stability index," in *IEEE PES Power Systems Conference and Exposition*, Atlanta, GA, pp. 1029–1036, 2006.

[22] M. H. Hussain, S. R. A. Rahim, and I. Musirin, "Optimal overcurrent relay coordination: A review," *Procedia Engineering*, Vol. 53, pp. 332–336, 2013.

[23] V. A. Papaspiliotopoulos, G. N. Korres, N. G. Maratos, "A novel quadratically constrained quadratic programming method for optimal coordination of directional overcurrent relays," *IEEE Transactions on Power Delivery*, Vol. 32, No. 1, pp. 3–10, Jul. 2017.

[24] Y. Damchi, M. Dolatabadi, H. R. Mashhadi, and J. Sadeh, "MILP approach for optimal coordination of directional overcurrent relays in interconnected power systems," *Electric Power Systems Research*, Vol. 158, pp. 267–274, May 2018.

[25] F. A. Albasri, A. R. Alroomi, and J. H. Talaq, "Optimal coordination of directional overcurrent relays using biogeography-based optimization algorithms," *IEEE Transactions on Power Delivery*, Vol. 30, No. 4, pp. 1810–1820, Feb. 2015.

[26] J. Radosavljević and M. Jevtić, "Hybrid GSA-SQP algorithm for optimal coordination of directional overcurrent relays," *IET Generation, Transmission & Distribution*, Vol. 10, No. 8, pp. 1928–1937, May 2016.

[27] A. Srivastava, J. M. Tripathi, S. R. Mohanty, and B. Panda, "Optimal over-current relay coordination with distributed generation using hybrid particle swarm optimization–gravitational search algorithm," *Electric Power Components and Systems*, Vol. 44, No. 5, pp. 506–517, Feb. 2016.

[28] V. N. Rajput, F. Adelnia, K. S. Pandya, "Optimal coordination of directional overcurrent relays using improved mathematical formulation," *IET Generation, Transmission & Distribution*, Vol. 12, No. 9, pp. 2086–2094, May 2018.

[29] ALSTOM, *Network protection & automation guide*. Ithaca, NY: Cornell University, pp. 1–497, 2010.

[30] C. Cortes and V. Vapnik, "Support-vector networks," *Machine Learning*, Vol. 20, No. 3, pp. 273–297, Sep. 1995.

[31] H. Drucker, C. J. C. Burges, L. Kaufman, A. J. Smola, and V. Vapnik, "Support vector regression machines," *Advances in Neural Information Processing Systems*, Vol. 9, pp. 155–161, 1996.

[32] R. D. Zimmerman and C. E. Murillo-Sanchez, MATPOWER (Version 7.0) [Software], 2019, Available: https://matpower.org.

[33] R. Storn and K. Price, "Differential evolution - A simple and efficient heuristic for global optimization over continuous spaces," *Journal of Global Optimization*, Vol. 11, No. 4, pp. 341–359, Dec. 1997.

A. H. Poursaeed was born in Khorramabad, Iran, in 1993. He received B.Sc. and M.Sc. degrees from Lorestan University (LU), Khorramabad, Iran in 2015 and 2018, respectively. He is currently a Ph.D. Student at Lorestan University, Khorramabad, Iran. His research interests include power system dynamics and stability, electromagnetic transients, and machine learning applications in power systems.

F. Namdari received B.Sc. in Electrical Power Engineering from the Iran University of Science and Technology (IUST) in 1995, M.Sc. from Tarbiat Modarres University (TMU) in 1998, and Ph.D. from the IUST in 2006, all in Electrical Power Engineering. In 2003, for 11 months he worked as an Honorary Research Associate with Queen's University, Belfast, UK. From 2009 he joined Lorestan University, where he is now working as an Associate Professor. Since 2014, Dr. Namdari is an IEEE member. Dr. Namdari has published more than 90 technical papers in valuable journals and conferences. His fields of interest are power system protection, smart grids, power system transients, power system optimization, and wide-area monitoring, protection, and control of power systems.